THE NPOESS VIIRS DAY/NIGHT VISIBLE SENSOR

BY THOMAS E. LEE, STEVEN D. MILLER, F. JOSEPH TURK, CARL SCHUELER, RICHARD JULIAN, STEVE DEYO, PATRICK DILLS, AND SHERWOOD WANG

The VIIRS sensor on the upcoming NPOESS satellites will have an improved day/night visible channel to image the earth and atmosphere at all levels of illumination.

The National Polar-orbiting Operational Environmental Satellite System (NPOESS) represents the next-generation U.S. operational polar satellite constellation. Designed to monitor the global environment, including the atmosphere, oceans, land surfaces, and sea ice, the NPOESS program is overseen by the Integrated Program Office (IPO), a multiagency group comprising the Department of Defense, Department of Commerce, and the National Aeronautics and Space Administration (NASA). NPOESS consolidates civilian and military environmental sensing programs and expertise under a single national system.

The Visible–Infrared Imager–Radiometer Suite (VIIRS) is the next-generation radiometer slated to fly on the NPOESS series (scheduled for ~2010) and the NPOESS Preparatory Project (NPP) satellite (likely in ~2008). VIIRS draws from the best capabilities of contemporary operational and research observing systems to support tomorrow's operational constellation. The 22 channels featured on VIIRS are derived primarily from three legacy instruments: the National Oceanic and Atmospheric Administration (NOAA) Advanced Very High Resolution Radiometer (AVHRR), the NASA Moderate Resolution Imaging Spectroradiometer (MODIS), and the Defense Meteorological Satellite Program (DMSP) Operational Linescan System (OLS). With a low-light nighttime visible sensing capability, the OLS is the only sensor providing technology heritage for the VIIRS Day/Night Band (DNB). Table 1 summarizes the VIIRS imaging resolution (I) channels, moderate resolution (M) channels, and the DNB (the DNB spatial resolution is explained further in the "NPOESS VIIRS DNB overview"). Table 1 represents pixel dimensions in the along- and cross-track directions. Some of the moderate channels have dual gains, capable of measurement within two discrete ranges of radiance (Table 1). The nadir spatial resolution of the dual-gain channels will be converted to the resolution of the other moderate channels (0.742 km × 0.776 km) by ground processing.

AFFILIATIONS: LEE, MILLER, AND TURK—Naval Research Laboratory, Monterey, California; SCHUELER AND JULIAN—Raytheon Corporation, Santa Barbara, California; DEYO, DILLS, AND WANG—UCAR/COMET, Boulder, Colorado
CORRESPONDING AUTHOR: Thomas F. Lee, Naval Research Laboratory, 7 Grace Hopper Ave., Monterey, CA 93943
E-mail: lee@nrlmry.navy.mil

The abstract for this article can be found in this issue, following the table of contents.
DOI:10.1175/BAMS-87-2-191

In final form 22 August 2005

Table 1. VIIRS channels.			
Band number/gain	VIIRS wavelength (μm)	VIIRS nadir pixel size along track × cross track (km)	Primary application
M1, dual	0.412	0.742 × 0.259	Ocean color, aerosols
M2, dual	0.445	0.742 × 0.259	Ocean color, aerosols
M3, dual	0.488	0.742 × 0.259	Ocean color, aerosols
M4, dual	0.555	0.742 × 0.259	Ocean color, aerosols
I1, single	0.640	0.371 × 0.387	Imagery, vegetation
M5, dual	0.672	0.742 × 0.259	Ocean color, aerosols
M6, single	0.746	0.742 × 0.776	Atmospheric correction
I2, single	0.865	0.371 × 0.387	Vegetation
M7, dual	0.865	0.742 × 0.259	Ocean color, aerosols
DNB, multiple	0.7	0.742 × 0.742	Imagery
M8, single	1.24	0.742 × 0.776	Cloud particle size
M9, single	1.38	0.742 × 0.776	Cirrus cloud cover
M10, single	1.61	0.742 × 0.776	Snow fraction
I3, single	1.61	0.371 × 0.387	Binary snow map
M11, single	2.25	0.742 × 0.776	Clouds
M12, single	3.70	0.742 × 0.776	Sea surface temperature (SST)
I4, single	3.74	0.371 × 0.387	Imagery, clouds
M13, dual	4.05	0.742 × 0.259	SST, fires
M14, single	8.55	0.742 ×0.776	Cloud-top properties
M15, single	10.76	0.742 × 0.776	SST
I5, single	11.45	0.371 × 0.387	Cloud imagery
M16, single	12.01	0.742 × 0.776	SST

This paper examines the DNB, just one of the many new capabilities of NPOESS sensor technology. For background, the following section gives an overview of the existing nighttime capability provided by the DMSP OLS. The "NPOESS VIIRS DNB overview" compares these current capabilities with those anticipated with the DNB. The "Detection of features as a function of lunar phase" section outlines some of the fundamental physical considerations for nighttime visible applications. The section titled "Lunar reflection applications" discusses applications requiring lunar illumination, including snow cover, airborne dust, smoke, and clouds. The "Emission-based applications" section covers features that can be identified through their own emission characteristics, such as city lights, fires, and lightning.

DMSP OLS OVERVIEW. Although the U.S. Air Force (USAF) has operated the DMSP OLS (Johnson et al. 1994; Elvidge et al. 1996, 1998b) since the late 1960s, data were not publicly available until the program's declassification in 1973 (Croft 1978). The particular goal of the nighttime visible channel on the OLS was to extend the daytime capability of cloud cover mapping to moonlit conditions. The National Geophysical Data Center (NGDC) has recently made available global digital archives of OLS data from the last decade, opening a resource once restricted by the U.S. Department of Defense.

The OLS consists of three instruments: telescopes for the visible (VIS) and infrared (IR) bands, and a photomultiplier tube for the nighttime visible band, all imaging in 3000-km swaths. The nighttime VIS channel actually covers a portion of both the VIS and near-IR regions of the electromagnetic spectrum (Elvidge et al. 1998a). The VIS data are partitioned into a limited 64 levels of gray, and the IR into 256 levels. The lack of calibration and coarse radiometric resolution available on OLS limits its utility in quantitative environmental applications. It is important to recognize that the OLS was designed as an imager to create simple imagery for human interpretation, explaining the relatively

few levels of gray. The civilian NOAA AVHRR, on the other hand, was designed as a calibrated radiometer to provide scientific observations with data partitioned into 1024 gray levels.

The OLS nighttime band is designed to be sensitive over a large range of cloud illumination. At the high end of the illumination range, the sensor measures reflected solar radiance at the day/night terminator. At a lower level it is able to detect clouds under full-moon conditions in the night sky. It can sometimes detect clouds under a partial moon, or a moon low in the night sky. With sufficient moonlight, snow cover, smoke, airborne dust, sea ice, and land surface features can also be detected. In the absence of illumination by light from below, no clouds are seen when the moon, regardless of phase, is below the horizon. To accommodate for this large range of illumination, an automatic gain is applied to normalize the data for viewing. Using a photomultiplier tube, the VIS signal is enhanced at night, making it possible to detect low emissions from lights, fires, lava flows, and gas flares. There are two main spatial resolutions, a smooth mode at 2.7 km and a fine mode at 0.56 km. These figures overstate the ability of the sensor to produce effective VIS images at night. This discrepancy occurs because the instantaneous field of view (IFOV) of the nighttime sensor is much larger than the nominal footprint size, leading to substantial pixel overlap. The large, overlapping IFOVs greatly limit the sharpness and detail of DMSP OLS nighttime images. Fortunately, the OLS technology employs a number of strategies to restrain the IFOV as a function of scan angle. The IFOV ranges from 2.2 km at subpoint to 4.2 km at 766 km out from the nadir. Then, after a switch in aperture, the IFOV is reduced to 3.0 km, rising to 5.4 km at the edge of scan (Elvidge 1998b).

NPOESS VIIRS DNB OVERVIEW. The DNB will measure VIS radiances from the Earth and atmosphere (solar/lunar reflection and both natural and anthropogenic nighttime light emissions) during both day and night portions of the orbit. In comparison to the OLS, some of the DNB channel improvements include 1) reduced instances of pixel saturation, 2) a smaller IFOV, leading to reduced spatial blurring, 3) superior calibration and radiometric resolution, 4) collocation with multispectral measurements on VIIRS and other NPOESS sensors, 5) and generally increased spatial resolution and elimination of cross-track pixel size variation.

The DNB is implemented as a dedicated focal plane assembly (FPA) that shares the optics and scan mechanism of the other VIIRS spectral bands. This integral design approach offers lower overall system complexity, cost, mass, and volume compared to a separate DNB sensor. Unlike the OLS, the DNB will feature radiometric calibration, with accuracy comparable to the other VIIRS spectral bands.

To achieve satisfactory radiometric resolution across the large dynamic range (seven orders of magnitude) of day/night radiances encountered over a single orbit, the DNB selects its amplification gain dynamically from three simultaneously collecting stages (groups of detectors residing upon the same FPA). The stages detect low-, medium-, and high-radiance scenes with relative radiometric gains of 119,000:477:1 (high:medium:low gain). Each of the three stages covers a radiance range of more than 500:1, so that the three together cover the entire required radiance range with generous overlap. Two identical copies of the high-gain stage are provided, which improves the signal-to-noise ratio (SNR) at very low signal levels and allows for the correction of pixels impacted by high-energy subatomic particles. The scene is scanned sequentially such that each scene is imaged by all three gains virtually simultaneously.

The signals from all gain stages are always digitized, using 14 bits (16,384 levels) for the high-gain stage and 13 bits (8,192 levels) for the medium- and low-gain stages. This fine digitization assures that the DNB will have much finer radiometric resolution than OLS across the entire dynamic range. Logic in the VIIRS Electronics Module (EM) then selects, on a pixel-by-pixel basis, the most appropriate of the three stages to be transmitted to Earth. In general, the VIIRS EM logic chooses the most sensitive stage in which the pixel is not saturated. This imaging strategy produces nonsaturated calibrated radiances in bright areas, and data with a lower dynamic range in the darkest areas with less SNR and radiometric accuracy. The raw data can then be converted by postacquisition processing into "constant contrast" imagery, meaning that an entire scene will appear as if it were uniformly illuminated. Fortunately, the brightness transitions between pixels processed with different gain stages should be relatively low, and users will probably not notice variations on images. The distracting effects of nonuniform illumination will be mitigated even for the day/night terminator scenes, in which the darkest night is divided from daylight.

The sensitive area of each charge-coupled device (CCD) stage is made up of multiple detector elements, each of which is smaller than the area needed to image a full DNB scene pixel. The CCD aggregates the signals from groups of these subpixel detectors in both the along- and cross-track directions to create an effec-

tive detector that maintains a nearly constant IFOV across the scan. The angular IFOV is relatively large at nadir, and narrower at the edge of the scan, such that the effective detector footprint projected on the Earth's surface will be essentially constant both along and cross track at 742 m (±5%) over the entire swath. This achieves nearly constant spatial resolution across the entire swath such that images will be equally sharp at nadir and at the edge of scan. Thus, compared to the OLS smooth mode (used to produce the examples shown in the "Lunar reflection applications" and "Emission-based applications" sections), the improvement in resolution (defined as pixels per unit area) is about 14 times near nadir (0.74-km pixels for VIIRS versus 2.8-km pixels for OLS) and about 53 times at the edge of scan (5.4-km pixels for OLS). The maintenance of constant resolution comes at the expense of some decrease in SNR away from nadir. But even at the edge of scan, the SNR performance will exceed the nadir requirement originally specified by the NPOESS IPO.

DETECTION OF FEATURES AS A FUNCTION OF LUNAR PHASE. Similar to the OLS, the ability of the DNB to detect specific features will be a strong function of lunar illumination. The amount of moonlight available to illuminate clouds and the surface of the Earth depends on both lunar phase (ranging from a new to full moon) and lunar elevation in the sky. The amount of lunar illumination provided by the moon is not a linear function of the lunar phase, due in part to the fact that shadows produced by lunar topography (e.g., craters, ridges, etc.) are minimized at full moon. The intensity of illumination is about 9 times greater at full moon than at the first- or third-quarter moon. Surprisingly, the moon is not an efficient reflector of solar energy, with an albedo of about 0.07 versus 0.39 for the Earth; the perceived brightness to our eyes is exaggerated by the contrast of the moon against the dark space background.

Virtually all reflective earth scene features at night will fall within the dynamic range of the most sensitive (high-gain) DNB stage. As indicated in the conceptual illustration shown in Fig. 1a, clouds, fog, land surfaces, snow cover, and smoke/ash clouds will be readily detectable through moonlight reflection. Sources of light emission (e.g., fires, lightning, city lights, gas flares, brightly lit fishing boats, and lava flows) will also be seen. However, because of the low gain and the presence of lunar reflection, these discrete emission sources will appear relatively faint compared to moon-free conditions. For a quarter-moon or less, features requiring illumination will become difficult to detect, and will disappear altogether when moonlight is absent (Fig. 1b). The fine quantization of the high-gain signals will enhance the appearance of terrestrial and atmospheric light emissions, including faint city lights and the aurora, while the pixel-by-pixel selection of gain stages ensures that even the brightest of city lights will not saturate the DNB.

LUNAR REFLECTION APPLICATIONS. *Snow, ice, and clouds.* VIS satellite sensors provide one of the few current means to observe and map snow and ice cover operationally (e.g., Ramsay 1998). Most VIS sensors have only the capacity for daytime measurements, limiting observation during winter when nights are long. This season matches the time of greatest need for accurate snow cover observations in many regions. The problem becomes extreme near the poles where Arctic (Antarctic) night prevails during the winter. Infrared and passive microwave sensors also have the capability to observe snow cover, but have several limitations. For example, IR sensors often fail to detect snow cover because of the lack of thermal contrast inherent in many winter scenes at night. Passive microwave sensing is hampered by a large footprint size that fails to delineate the boundaries of snowfields well. Thus, moonlit VIS images can potentially satisfy an important need (Foster 1983; Foster and Hall 1991) that will be demonstrated when NPOESS VIIRS comes online.

Figure 2a, a nighttime OLS IR image, shows a mixture of clouds and clear skies over the Midwest. Snow covers parts of Iowa, Kansas, and Missouri, but cannot be seen well because of the lack of thermal contrast with the cold land background. The OLS nighttime color composite (Fig. 2b), which combines nighttime VIS data with OLS IR data, distinguishes the surface from the clouds. Snow cover is shown in white, cloud-free land in blue, clouds in yellow,

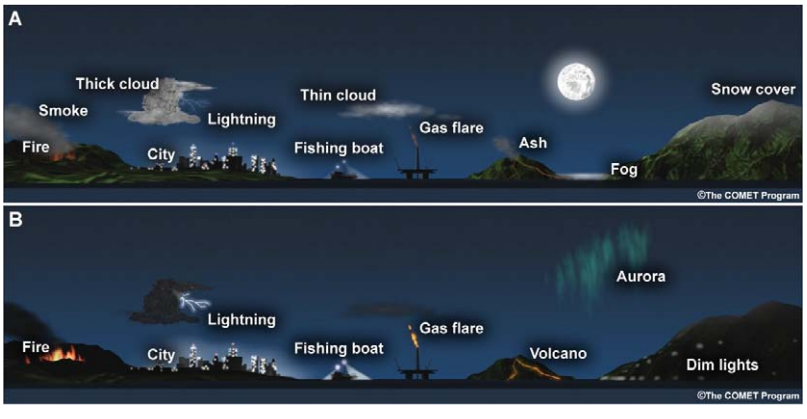

Fig. 1. Nighttime visible detection capabilities (a) with and (b) without lunar illumination.

and cities in magenta. A MODIS cloud-over-snow enhancement (Fig. 2c; following Miller et al. 2005) validates the OLS-defined snow swath in white. With the onset of VIIRS, the DNB, in combination with longwave and shortwave IR channels, will improve snow detection and further enhance nighttime snow cover products. The coarse appearance of products such as Fig. 2b will be greatly improved.

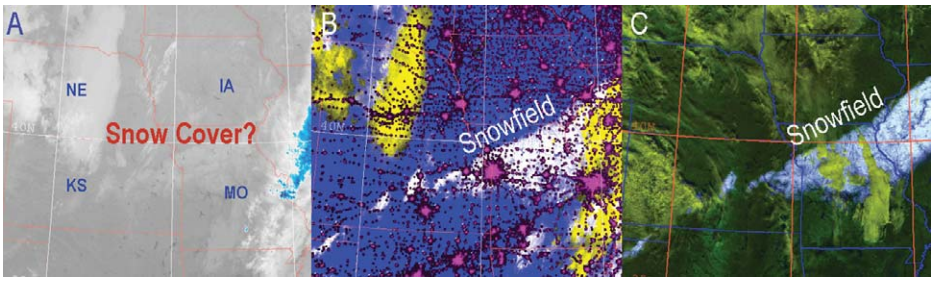

Fig. 2. Snow cover detection: (a) DMSP OLS (F-15) IR over the central United States at 0301 UTC 25 Nov 2004, (b) same pass as in (a), except for nighttime IR/VIS combination; snowfield appears in white, clouds mostly in yellow, and cities in magenta. (c) corresponding MODIS *Terra* snow–cloud product the next day (at 1720 UTC 25 Nov 2004); snow in white, clouds in yellow, land in dark green.

Airborne dust, low cloud, and smoke detection. Under sufficient moonlight, the DNB will be able to detect blowing and suspended dust at night. Other satellite sensors generally fail to detect dust at night due to lack of contrast between dust and the surface IR channels. Using daytime MODIS data (Miller 2003), Fig. 3a shows a large Saharan dust storm advancing southwestward across western Africa. Figure 3b shows the same dust storm at night imaged by the DMSP OLS 9 h later, enhancing the reflective land and overlying dust to emphasize the advancing dust front (yellow shades). While Fig. 3b shows a capability to depict a strong dust event with ample moonlight, a large number of other dust events cannot be resolved in OLS nighttime images due to weaker reflection and coarse radiometric resolution. With 16,384 gray shades (compared to 64 on the OLS), higher spatial resolution, and the support of multispectral observations, the VIIRS DNB will enable a much-improved nighttime dust product.

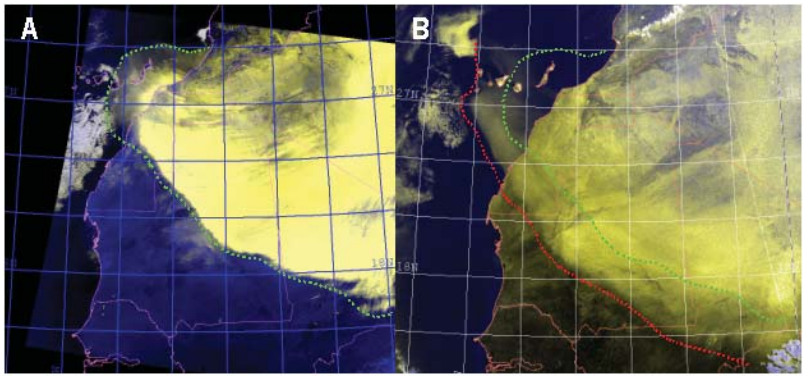

Fig. 3. Airborne dust detection: (a) *Terra* MODIS daytime dust product at 1110 UTC 3 Mar 2004. Dust (yellow) is advancing toward the west-southwest through the Sahara Desert (leading edge marked by a green line). (b) DMSP OLS (F-16) nighttime IR/VIS combination enhanced for dust detection at 2017 UTC 3 Mar 2004. Advance of dust front compared to the earlier MODIS product is shown (red line).

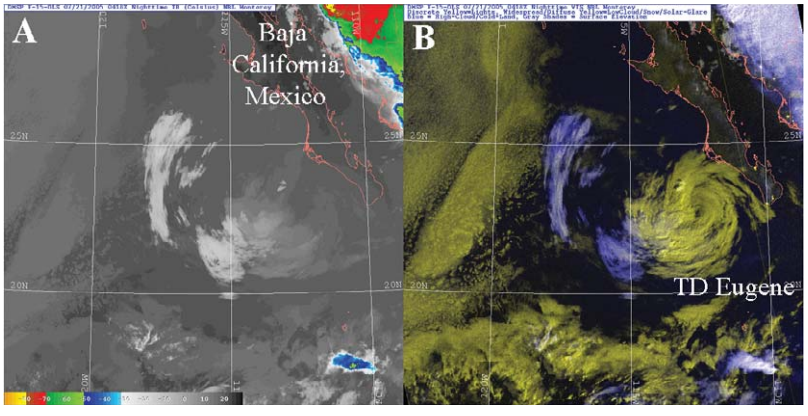

Fig. 4. (a) Low clouds at night: DMSP OLS (F-15) nighttime IR at 0418 UTC 21 Jul 2005. (b) IR/VIS combination, where low clouds are yellow and high clouds are blue.

Nighttime low clouds and fog, which usually blend in with the thermal background on IR images, pose a detection problem in a number of settings, including weak tropical cyclones. For example, in Figure 4, the IR image on the left shows only curved cirrus streaks associated with eastern Pacific Tropical Depression (TD) Eugene (estimated maximum sustained winds of 25 kt). Techniques relying on both longwave and shortwave IR channels can detect low clouds at night (e.g., Lee et al. 1997). However, they sometimes fail if the low clouds are composed of large droplets, if thin cirrus is present, or

if the surface temperature is well below freezing. Figure 4b, a VIS/IR DMSP OLS composite, shows the low-cloud circulation associated with Eugene in yellow and the cirrus streaks in blue. In addition, Figure 4b reveals a large stratus field to the west (yellow), which is also difficult to detect in the stand-alone IR image (Fig. 4a). Algorithms using VIIRS will draw upon the strengths of both the DNB and infrared channels for a greatly improved depiction of clouds at night.

Monitoring of moonlit smoke plumes from fires is likely to become a major application of the VIIRS DNB. It should lead to improved forecasts of air quality (a high-priority initiative within the U.S. National Weather Service and the Environmental Projection Agency). With DMSP OLS, however, this detection capability is marginal due to the relatively poor sensitivity of the instrument, the coarse spatial resolution of the available images (generally "smooth" as described in the "DMSP OLS overview"), and the difficulty in acquiring timely data. In late June 2002 the Chediski-Rodeo fire, one of the most intense wildfires in state history, raged for days over the eastern Arizona. The OLS nighttime VIS sensor detected the smoke (Fig. 5) emanating from a visible fire signature (fire signatures are examined further in the following section).

EMISSION-BASED APPLICATIONS. *City lights and wildfire detection.* The first USAF meteorologists to view OLS nighttime VIS imagery were amazed to observe bright clusters on the images corresponding to locations of known cities. These lights were particularly prominent under higher-gain settings (applied in conditions of little or no moonlight), but were more difficult to see under lower-gain settings (full moon). Since DMSP OLS declassification, published research has focused on the mapping of anthropogenic lights on the Earth's surface, especially from cities (Sullivan 1989; Elvidge et al. 1998b). The cities can often be seen through cloud structures, though sometimes with distorted shapes (Croft 1978). While the ability to see dim lights is greatest in periods without moon, most city lights can also be observed in moonlit conditions (e.g., Fig. 5). Spectacular global composites of city lights are one of the hallmark products of the OLS sensor (Sullivan 1989). VIIRS DNB was not specifically designed to improve the imaging of light sources on the surface of the Earth. Nevertheless, it is likely that many more lights will be detected due to a smaller footprint size, higher SNR, and greatly increased radiometric resolution.

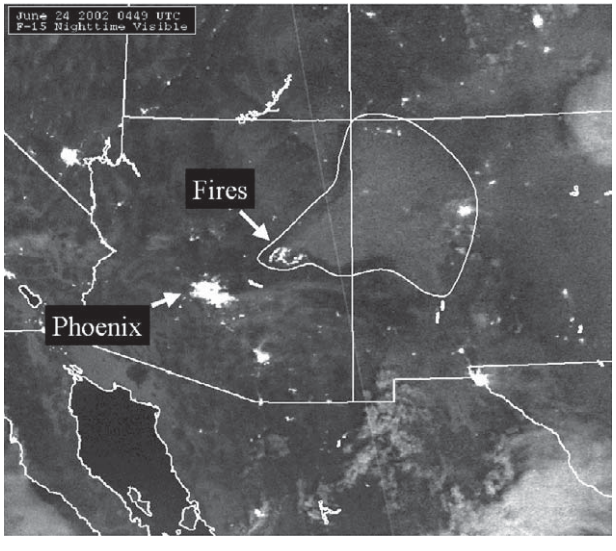

Fig. 5. Smoke detection under moonlight in the southwestern United States. DMSP OLS (F15) nighttime VIS at 0449 UTC 24 Jun 2002. Curved white enclosure expanding to the east of the fire zone delineates smoke.

Fires can be detected from the OLS at night (Elvidge et al. 1997, 1998a; Fuller and Fulk 2000) based on the identification and screening of lights from known fire sources (Elvidge et al. 1998b). But OLS is not widely used in research or operational fire-detection and classification algorithms. Instead, detection algorithms rely on fully calibrated, multispectral data from the NOAA AVHRR, MODIS, and Geostationary Operational Environmental Satellite (GOES) imager, especially channels within the 3.7–3.9-μm (shortwave IR) region, which are sensitive to extreme heat and therefore wildfires. VIIRS will offer the advantage of having both shortwave IR and improved nighttime VIS channels on the same instrument. The combination will be able to confirm the presence of fires and provide estimates of their size and intensity.

Under a moonless sky, a DMSP OLS image (Fig. 6a) reveals the light of major urban regions in coastal southern California. Included among these lights are flames from a group of large wildland fires raging through the backlands. However, they cannot be distinguished from nearby urban lights. To isolate the fires, we performed a pixel-by-pixel subtraction of the image containing the fires from the background image without fires. The city-light pixels are removed, leaving the fire pixels in red (Fig. 6b). The locations of the fires are confirmed by daytime a MODIS *Terra* true color image 14 h later (Fig. 6c), annotated with fire positions derived from the MODIS 3.7-μm channel. Active flames are responsible for the fire signatures in Fig. 6b. Together with two accompanying shortwave infrared channels that are sensitive to heat (at or near 3.7 μm), VIIRS DNB will be able to detect both active "crowning" fire regions as well as cooler smoldering areas.

Lightning. While low IR brightness temperatures are often used to identify thunderstorms in satellite imagery, the exact location of convective towers may be obscured by anvil cirrus exhibiting similar temperatures. The loca-

tion of strikes from a lightning-detection network gives more precise information about these embedded cells, but is available only where an extensive surface observing network has been established.

Figure 7a shows a springtime nocturnal squall line over Texas. While the general extent of the storm is identified through its cold brightness temperatures (white), it is difficult to distinguish active convection from stratiform rainfall regimes based on the IR image alone. Lightning strikes from the National Lightning Detection Network (NLDN) indicate the presence of a convective line embedded within this storm complex whose orientation is not obvious from the IR brightness temperature field structure alone. The DMSP OLS image (Fig. 7b) identifies the same convective line as a series of bright streaks (Orville 1981; Orville and Henderson 1986). The streaks usually do not depict the lightning discharge itself, but are artifacts of the flicker of the storm tops (through multiple scattering and diffusion of the lightning flash through the cloud) as the OLS detector scans the vicinity of a lightning strike. We believe that the VIIRS DNB instrument will possess a similar lightning-detection capability, useful in confirming the presence of electrically active storms worldwide, especially in remote areas and outside the range of lightning-detection networks.

SUMMARY AND CONCLUSIONS. The VIIRS DNB will bring significant advances to operational and research applications at night. Spatial resolution will be improved, and restrained pixel growth will preserve image quality toward the edge of the swath. The strategy of dynamic gain selection will ensure imagery of a high and uniform quality under a variety of lunar illumination levels. SNR will be

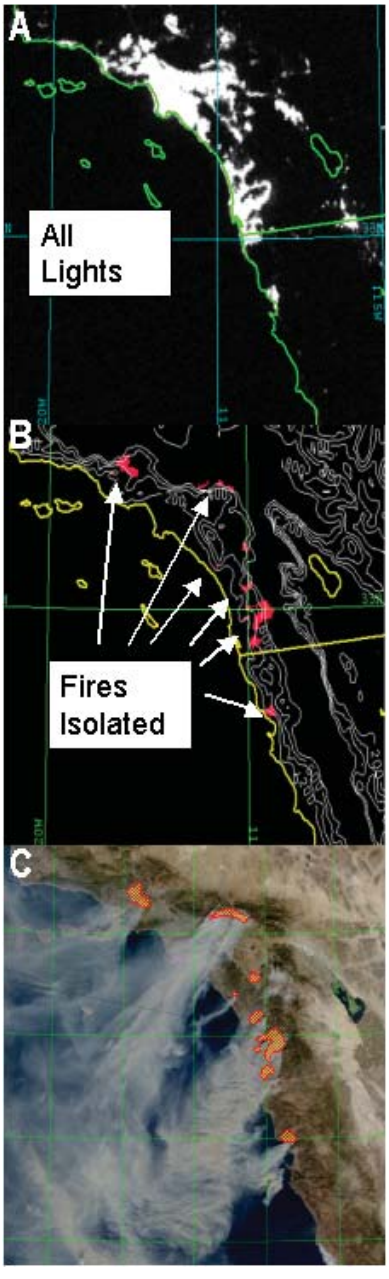

FIG. 6 (LEFT). Active fire detection over southern California: (a) DMSP OLS (F15) nighttime VIS at 0424 UTC 26 Oct 2003. (b) Same satellite as in (a), but processed to isolate fires. (c) MODIS *Terra* fire product the next day (fire perimeters indicated in red) at 1840 UTC 26 Oct.

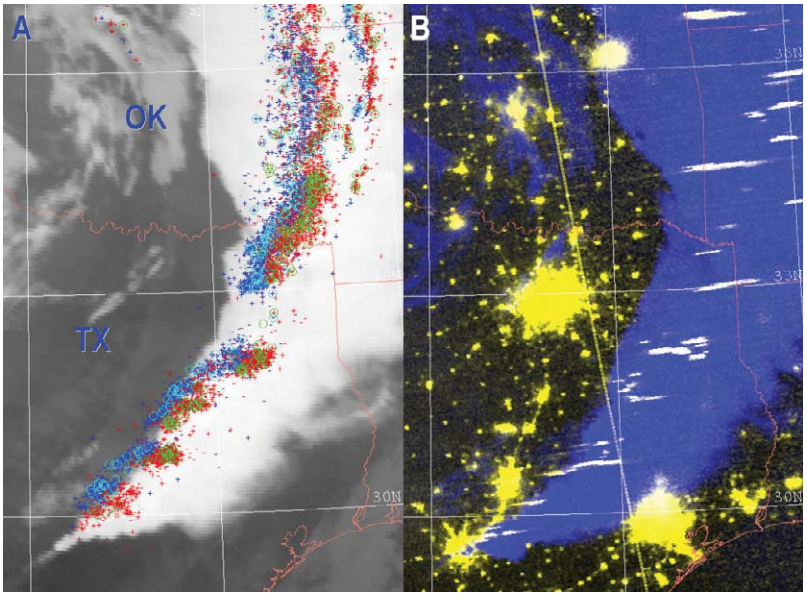

FIG. 7 (ABOVE). Lightning detection over Texas: (a) GOES-East IR imagery at 0245 UTC 6 Apr 2004, with NLDN lightning strike observations overlaid (symbols: red = all strikes within the last 30 min relative to satellite collection time; green circles = intra-cloud strikes detected within the last 30 min; dark blue = all strikes 30–60 min old; cyan circles = intra-cloud strikes 30–60 min old). Positive/negative symbols designate strike polarity. Cold thunderstorm cloud tops are shown in white. (b) DMSP OLS (F-15) nighttime IR/VIS combination at 0302 UTC 6 Apr 2004. Cold cloud tops are dark blue. White streaks are lightning detected by the OLS. The city lights of Houston, San Antonio, Austin, Dallas, and Ft. Worth, TX, appear prominently. [NLDN data courtesy of Vaisala U.S. Lightning Detection Network.]

increased, improving image quality and quantitative applications. Like other VIIRS channels, the DNB will be radiometrically calibrated. It will provide very fine signal quantization, enabling features to be examined in quantitative detail.

Improvements with VIIRS DNB will vary with application. It will be possible to detect clouds, dust, and smoke ("Lunar reflection applications" section) at lower levels of lunar illumination with the DNB due to the increased sensitivity of the instrument. In cases of marginal illumination, information from other channels may confirm the existence of otherwise ambiguous clouds. Cloud and aerosol properties, such as optical depth and particle size, should be possible. Currently, satellite detection of snow cover at night is nearly impossible using available satellite remote sensing capabilities. The DNB, in concert with other channels upon VIIRS, will enable the discrimination of snow cover from both clouds and snow-free land. A variety of new nighttime snow cover products will complement daytime products.

VIIRS DNB images will reveal more numerous city lights due to increased spatial resolution and other factors ("Emission-based applications" section). Clouds are a major problem in the detection and study of cities using DMSP OLS, but VIIRS multispectral screening should help isolate true urban signatures. Also, detections of other anthropogenic signatures, including fishing boats and gas flares, will increase in density per unit area. Fire monitoring, aided by the detection of moonlit smoke, may be among the most significant applications using the DNB.

Near-real-time examples of DMSP OLS nighttime images can be viewed at the NexSat site, maintained by the Naval Research Laboratory (NRL) in Monterey, California (online at www.nrlmry.navy.mil/NEXSAT.html), for the continental United States. To anticipate VIIRS capabilities, including those of the DNB, online forecaster training has been developed (see www.meted.ucar.edu/npoess/viirs/) by the Cooperative Program for Operational Meteorology, Education, and Training (COMET).

ACKNOWLEDGMENTS. The support of the research sponsors, the Oceanographer of the Navy through the Operational Effects Program Office (PMW-180) under Program Element PE-0603207N, the Office of Naval Research under Program Element PE-0602435N, and the National Polar-orbiting Operational Environmental Satellite System's Integrated Program Office located in Silver Spring, Maryland, is gratefully acknowledged.

REFERENCES

Croft, T. A., 1978: Night-time images of the earth from space. *Sci. Amer.,* **239,** 86–98.

Elvidge, C. D., H. W. Kroehl, E. A. Kihn, K. E. Baugh, E. R. Davis, and W. M. Hao, 1996: Algorithm for the retrieval of fire pixels from DMSP Operational Linescan System Data. *Biomass Burning and Global Change: Remote Sensing, Modeling and Inventory Development, and Biomass Burning in Africa,* J. S. Levine, Ed., MIT Press, 73–85.

——, K. E. Baugh, E. A. Kihn, H. W. Kroehl, and E. R. Davis, 1997: Mapping of city lights using DMSP Operational Linescan System data. *Photogramm. Eng. Remote Sens.,* **63,** 727–734.

——, D. W. Pack, E. Prins, E. A. Kihn, J. Kendall, and K. E. Baugh, 1998a: Wildfire detection with meteorological satellite data: Results from New Mexico during June of 1996 using GOES, AVHRR and DMSP-OLS. *Remote Sensing Change Detection: Environmental Monitoring Methods and Applications,* R. S. Lunetta and C. D. Elvidge, Eds., Ann Arbor Press, 103–121.

——, K. E. Baugh, V. R. Hobson, E. A. Kihn, and H. W. Kroehl, 1998b: Detection of fires and power outages using DMSP-OLS data. *Remote Sensing Change Detection: Environmental Monitoring Methods and Applications,* R. S. Lunetta and C. D. Elvidge, Eds., Ann Arbor Press, 123–135.

Foster, J. L., 1983: Night-time observations of snow using visible imagery. *Int. J. Remote Sens.,* **4,** 785–791.

——, and D. K. Hall, 1991: Observations of snow and ice features during the polar winter using moonlight as a source of illumination. *Remote Sens. Environ.,* **37,** 77–88.

Fuller, D. O., and M. Fulk, 2000: Comparison of NOAA AVHRR and DMSP-OLS for operational fire monitoring in Kalimantan. Indonesia. *Int. J. Remote Sens.,* **21,** 181–187.

Johnson, D. B., P. Flament, and R. L. Bernstein, 1994: High resolution satellite imagery for mesoscale meteorological studies. *Bull. Amer. Meteor. Soc.,* **75,** 5–33.

Lee, T. F., F. J. Turk, and K. Richardson, 1997: Stratus and fog products using *GOES-8-9* 3.9-μm data. *Wea. Forecasting,* **12,** 664–677.

Miller, S. D., 2003: A consolidated technique for enhancing desert dust storms with MODIS. *Geophys. Res. Lett.,* **30,** 2071, doi:10.1029/2003GL018279.

——, T. F. Lee, and R. Fennimore, 2005: Satellite-based imagery techniques for daytime cloud/snow delineation from MODIS. *J. Appl. Meteor.,* **44,** 987–997.

Orville, R. E., 1981: Global distribution of midnight lightning—September to November 1977. *Mon. Wea. Rev.,* **109,** 391–395.

——, and R. W. Henderson, 1986: Global distribution of midnight lightning: September 1977 to August 1978. *Mon. Wea. Rev.,* **114,** 2640–2653.

Ramsay, B., 1998: The interactive multisensor snow and ice mapping system. *Hydrol. Process.,* **12,** 1537–1546.

Sullivan, W. T., III, 1989: A 10 km resolution image of the entire night-time earth based on cloud-free satellite photographs in the 400-1100 nm band. *Int. J. Remote Sens.,* **10,** 1–5.